26. Devanand, K. & Selser, J. C. Polyethylene oxide does not necessarily aggregate in water. *Nature* **343,** 739–741 (1990).
27. Model, P. & Russel, M. in *The Bacteriophages* (ed. Calender, R.) Ch. 6, 375–456 (Plenum, New York, 1988).
28. Chiruvolu, S., Naranjo, E. & Zasadzinski, J. A. *Microstructure of Complex Fluids by Electron Microscopy* (Am. Chem. Soc., Washington DC, 1994).

Acknowledgements. We acknowledge grant support from the NSF (D.M.R.)

Correspondence and requests for materials should be addressed to S.F. (e-mail: seth@smectic.elsie.brandeis.edu). Further information is available on the World Wide Web at http://www.elsie.brandeis.edu.

Low argon solubility in silicate melts at high pressure

Eva Chamorro-Pérez*, Philippe Gillet*, Albert Jambon†, James Badro* & Paul McMillan*‡

** Institut Universitaire de France, Laboratoire de Science de la Terre, CNRS UMR 5570, École Normale Supérieure de Lyon, 46 allée d'Italie, 69364 Lyon cedex 07, France*
† Laboratoire MAGIE, CNRS URA 1762, Université de Paris VI, 4 place Jussieu, 75252 Paris cedex 05, France

The solubility of rare gases in silicate melts and minerals at high pressure is of importance for understanding the early history of the Earth and its present day degassing. Helium, neon, argon, krypton and xenon were originally incorporated into the Earth during its accretion, and have also been produced by radioactive decay[1]. These elements have been used as tracers for deciphering mantle structure and constraining the number and size of geochemical reservoirs[1–3]. In particular, it has been proposed that the budget of ^{40}Ar, produced by the radioactive decay of ^{40}K, provides the strongest argument for chemical layering within the mantle[1,4]. The geochemical models used to arrive at this conclusion are, however, currently under re-examination[5], with a large source of uncertainty being the lack of data on argon partitioning during melting. It has previously been assumed, on the basis of low-pressure data, that noble gases are highly soluble in melts at all pressures. But here we present solubility data of argon in olivine melt at very high pressure that indicate that argon solubility is strongly dependent on pressure, especially in the range of 4–5 gigapascals.

Degassing throughout Earth history has taken place by melting accompanied by dissolution of noble gases in the melt, followed by ascent of melt and escape to the atmosphere. Several recent studies have focused on rare-gas solubility in melts at low pressure (below 2.5 GPa)[6–8]. Newly developed high-pressure diamond anvil cell (DAC) techniques now permit melting experiments on mantle materials in the presence of argon under deep-mantle conditions[9]. Preliminary experiments on pure SiO_2 melt yielded the surprising result that Ar solubility decreased markedly above 5 GPa. We have now obtained data for a natural olivine melt composition that provide a more realistic model for mantle melts.

Polished $100 \times 100 \times 20\ \mu m^3$ plates (Fig. 1a) of single crystalline San Carlos olivine (chemical composition 49wt% MgO, 41wt% SiO_2, 10wt% FeO) were loaded into a high-pressure DAC along with Ar as pressure medium[9]. Pressure was measured from the calibrated shift of the intense Raman lines of the crystal before heating[10]. This avoided a potential chemical reaction with the ruby chips usually used for pressure measurement. Samples were heated at pressures up to 11 GPa by using a focused CO_2 laser beam[11]. Forsterite melts congruently to at least 12.7 GPa (ref. 12). Melting was detected optically by the formation of droplets (Fig. 1b). The laser power was

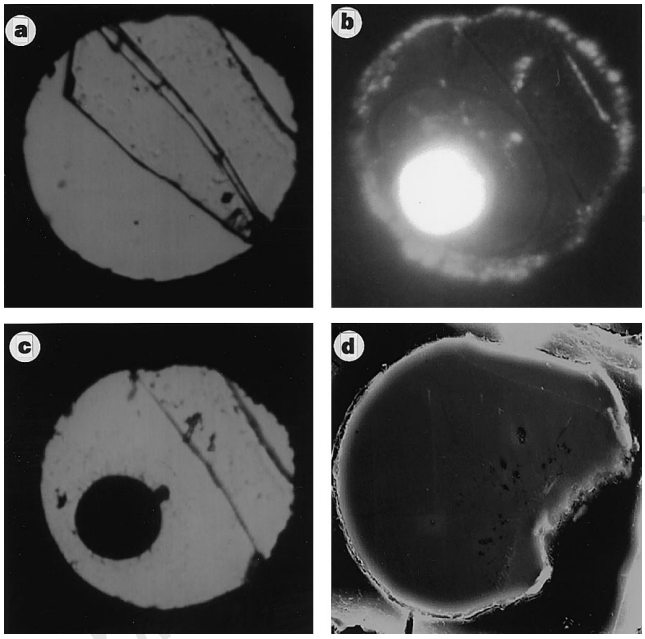

Figure 1 Series of optical micrographs taken through the diamonds of the DAC before and during the laser-heated experiment showing different stages of the high-pressure melting of olivine in the presence of Ar. **a**, Polished single-crystalline slab of San Carlos olivine compressed in solid Ar at 2.5 GPa before heating. The dark outline indicates the gasket hole in the diamond cell experiment. The largest dimension of the sample is 150 μm. The sample edges were fixed at two points of contact to the interior of the metal gasket. At ambient temperature and above 1.2 GPa, the Ar pressure-transmitting medium is solid. The line traversing the sample along its longest dimension is a fracture that occurred during compression. **b**, Photomicrograph of the sample *in situ* during laser heating at 2.5 GPa. The laser power was adjusted so that the temperature inside the molten spot was approximately 100–200 °C above the melting point. Only one piece of the fractured sample has melted to a spherical drop, and has moved away from the other half of the crystal (darker area above the melted spot). A rim of molten argon is visible around the hot bead of olivine melt: the Ar is solid elsewhere. **c**, Photomicrograph of the sample in the DAC after heating. When the laser power is cut, the molten sample quenches rapidly to glass (verified by polarized optical microscopy and micro-Raman spectroscopy, and by SEM analysis of the etched surface after removal from the DAC; see the text). The quenched bead of glassy sample droplet is then decompressed and prepared for chemical analysis. **d**, SEM image of a typical polished sample after etching (1 min in 1 M HCl). The sample surface shows only a smooth glassy texture. No fracture lines or bubbles are observed in the regions that were subjected to chemical analysis with the electron microprobe. The Ar content was measured by energy-dispersive and wavelength-dispersive analysis in the electron microprobe (Cameca SX50) with an accelerating voltage of 15 kV, a beam current of 100 nA and a counting time of 10 s on peak and background. The standard used was an SiO_2 glass containing 1wt% Ar. The Ar signal was measured simultaneously with two spectrometers. The electron beam was defocused to 5 μm in diameter to improve counting statistics on the low rare-gas content. The beam was rastered automatically across the sample surface in 5 μm steps. The reported Ar contents represent an average of approximately 20 points, depending on the sample analysed. A few empty 'bubbles' are visible on the right side of this sample: these are areas where the molten sample was 'pulled away' from the crystalline olivine during initial heating. These areas were avoided during the chemical analyses. All glassy samples analysed in this study formed monolithic blocks that remained intact during removal from the DAC, mounting in epoxy, and polishing. There was no evidence for microcracks or bubbles that might indicate decrepitation, for any of the glassy samples described here. Etching the sample surface did not reveal any additional texture that might indicate the presence of grain boundaries or other features associated with crystallization during the quench. Micro-Raman spectra of quenched samples occasionally showed the two most intense peaks of crystalline olivine superimposed on the broad bands of the glassy sample; however, these were not present for all samples, and there was no systematic difference between samples with high and low Ar content.

‡ Present address: Department of Chemistry and Biochemistry and Center for Solid State Science, Arizona State University, Tempe, Arizona 852287, USA.

adjusted to give temperatures just above the melting line (2,300–2,700 K)[12]. During melting, the surrounding Ar melts by conduction, allowing the drop to move within the sample chamber (Fig. 1b). Samples were quenched by switching off the laser power, then removed from the DAC and polished for electron microprobe analysis (Fig. 1c). A conservative estimate with known thermal diffusivities of molten silicates gives the quench rate as at least 10^3 K s^{-1}. The actual quench rate is probably much higher, owing to radiative losses.

Chemical homogeneity was determined by elemental mapping at random points (>20) across the sample. In the regions analysed, no microcracks or argon-containing bubbles were detected by scanning electron microscopy (SEM) (Fig. 1d). Potential loss of Ar from the sample during quenching can be ruled out. Ar was found to be present in all the samples, and systematic chemical maps and profiles revealed no statistically significant variation of the Ar content from the core toward the edge of the sample, regardless of the pressure of the experiment. If diffusion of Ar had occurred one should have observed a systematic decrease in Ar concentration from the centre of the sample towards the edge, which did not occur. A further argument for no Ar loss is that thermal diffusivity was at least two orders of magnitude higher than chemical diffusivity (10^{-2} to 10^{-3} cm^2 s^{-1} compared with 10^{-5} cm^2 s^{-1}). With our most conservative estimate of quenching time (10^{-3} s) one finds that the typical diffusion length of Ar is much less than 1 μm, much smaller than the size of the sample.

The amount of incorporated argon increases smoothly with pressure up to 4–5 GPa, to reach a maximum of 0.2wt%, as expected from an extrapolation of previous work on other melts at lower pressure[6–8]. Beyond 5 GPa, the solubility decreases markedly, by an order of magnitude (Fig. 2). This behaviour is completely unexpected from previous studies on depolymerized melt compositions, but is consistent with our preliminary observation for SiO_2 (ref. 9). The surface textures of all samples analysed were identical, independently of run pressure. None of the samples revealed the presence of crystalline material by optical and SEM examination, even after etching (Fig. 1d). Weak features due to traces of forsterite were occasionally detected in micro-Raman spectra of quenched samples superimposed on broad glassy bands, but these were observed at all pressures, independently of Ar content. We conclude that our observations reflect a real change in Ar solubility in the melt at high pressure.

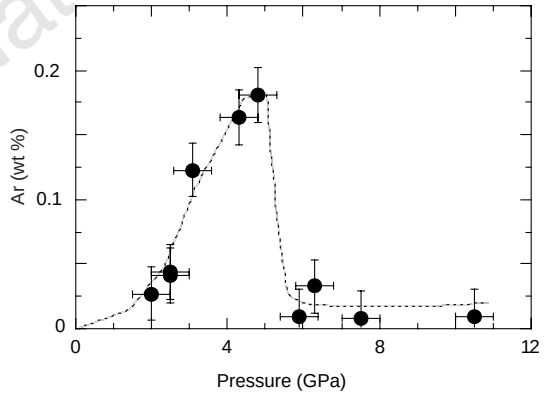

Figure 2 Argon solubility data for San Carlos olivine melt up to 10.5 GPa. Up to 4–5 GPa the solubility increases smoothly. Above this pressure a large decrease in solubility is observed. The dashed line does not represent a fit to the data, but is merely intended as a guide to the eye. It is obvious that a linear fit to these data would not yield a Henrian solubility behaviour passing through the origin, expected from previous work on high-silica melts at low pressure. This could indicate some deviation of the Ar solubility from ideality in the low-pressure range (<3 GPa), or it could be within the error of the data. Further discussion of this point must await Ar solubility determinations at low pressure.

Previous rare-gas solubility measurements at low pressures have been used to construct thermodynamic models for the dissolution process[8,13]. The models are based on the concept of 'ionic porosity', which describes the 'free' volume within the melt structure available to the chemically inert dissolving species, that is, the melt molar volume minus that occupied by the ions. The size distribution of available sites or 'holes' is determined from a series of solubility measurements with rare gases of different radii, and is described by the first moment of the distribution in a log–linear plot[13]. For a given melt, the hole size distribution is calculated from molar

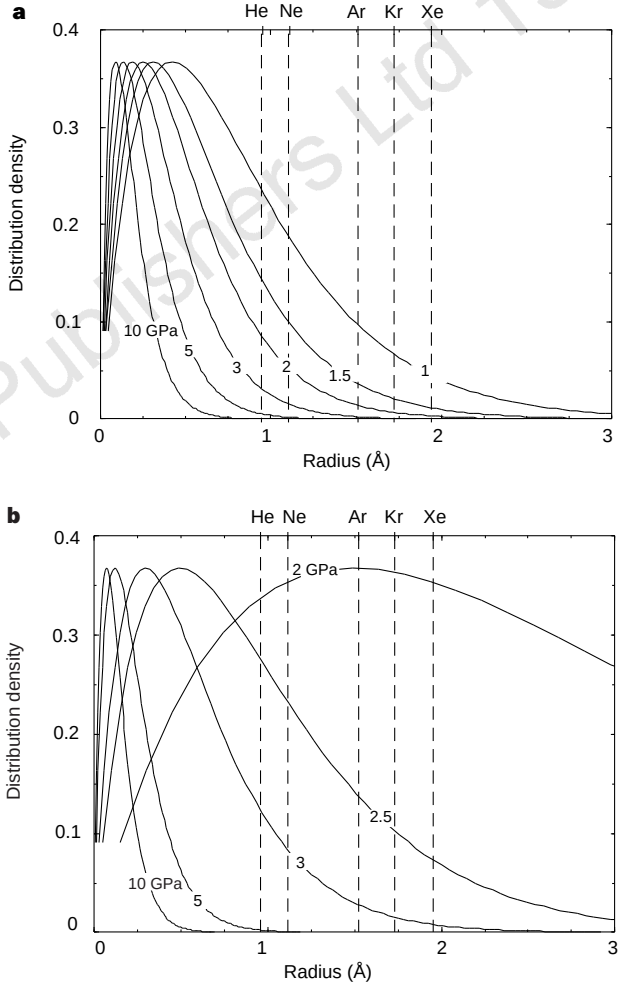

Figure 3 Hole size distribution in (**a**) olivine and (**b**) SiO_2 melts calculated with an ionic porosity model[8]. The distribution density is calculated with a log-linear model for site size probability[13]. The characteristic length coefficient is obtained by the slope of the measured solubility line against the atom radius for different rare gases. It is assumed that the decrease in ionic porosity and change in the hole size distribution is due only to a volume decrease of the melt with pressure, that is, that no major structural changes (such as coordination changes) occur in the melt over this pressure range. The change in volume for olivine melt is estimated with the following EOS parameters: $K_{TO} = 27$ GPa; $K' = 5$; $dK/dT = -5 \times 10^{-3}$ GPa/K; $\alpha_0 = 7 \times 10^{-5}$ K^{-1}; ionic volume (Mg + Fe + Si + O) = 27.44 cm^3/mol, molar volume at $P_0T_0 = 49.8$ cm^3/mol (ref. 15). The pressure dependence of the melting temperature of olivine has been included[12]. For SiO_2 we used the EOS published by Poole *et al.*[16]. The radii of the rare gases He, Ne, Ar and Xe are indicated on the axis. For Ar, it is observed that the tail of the hole size distribution in olivine decreases abruptly to near zero at a calculated pressure of 3–5 GPa, in good agreement with the experimental solubility measurements. Below this pressure the available sites are not completely filled, and the solubility model of Carroll and Stolper[8] applies. The analogous plot for SiO_2 is shown in (**b**). A similar interpretation holds for these data.

volume data and measured rare-gas solubilities. Over the pressure range considered by Carroll and Stolper[8], it was assumed that the available sites were never completely filled; this model predicts a Henrian solubility behaviour. At higher pressure it would be expected that all the available sites would become filled, and the solubility would reach a maximum value. This prediction stands in marked contrast to the abrupt drop in Ar solubility above 5 GPa observed here. However, if changes in the ionic porosity or hole size distribution with pressure are taken into account, a rapid decrease in rare gas solubility above a certain threshold pressure would be expected. Even in the absence of major structural changes within the melt[14], densification will cause a decrease in ionic porosity and change the distribution of the hole sizes (Fig. 3).

We have used an estimated equation of state (EOS) for molten olivine[15] to calculate ionic porosities over the pressure range of our measurements. At low pressure, the available sites for Ar are not completely filled, and the effect of pressure is to increase the solubility as observed (Fig. 2). At higher pressure, the ionic porosity is lowered to such an extent that the tail of the distribution is now markedly decreased in the size range of the argon atoms (Fig. 3a). The result of these competing effects is an initial increase in solubility with pressure, followed by a sudden decrease, as the range of available sites distribution crosses the Ar radius.

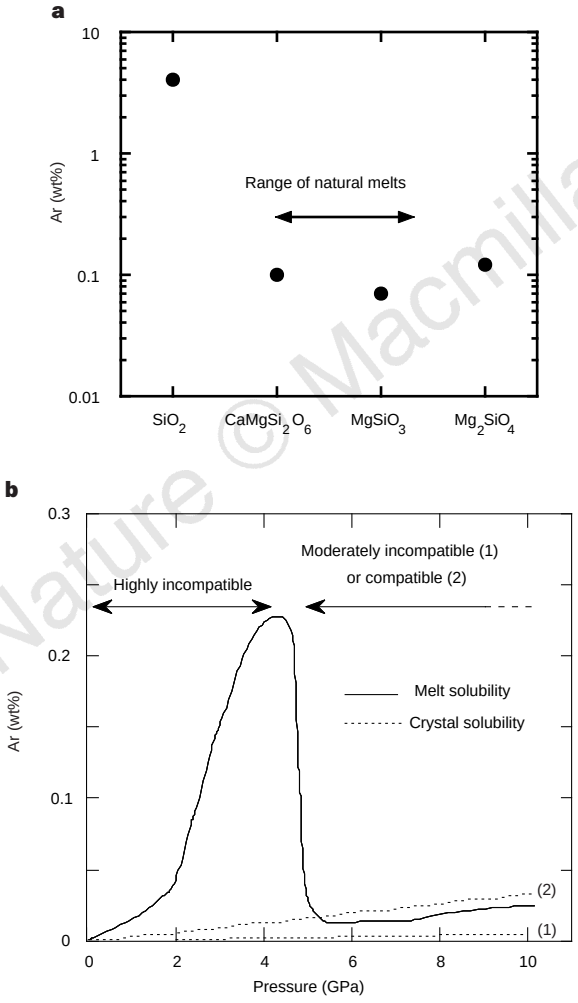

Figure 4 Solubility of argon in silicate melts as a function of composition and pressure. **a**, Argon solubility data at $P \approx 3$ GPa for SiO_2, diopside, enstatite and olivine melts. **b**. Comparison of Ar solubility in olivine melt measured as a function of pressure in this study with the expected solubility in crystalline olivine, obtained by extrapolating the low-pressure crystal–melt fractionation factor ($K_d \approx 10^{-2}$) to high pressure. Two possible Henry's-law crystal solubilities are shown, consistent with the low-pressure value of crystal–melt fractionation, within estimated limits of experimental error.

A similar argument can be used to explain the results previously observed for SiO_2 melt[9] (Fig. 3b). Here we use a melt EOS obtained from molecular dynamics simulation[16]. The evolution of the pore size distribution with pressure is similar to that for olivine melt. This rationalizes why the Ar solubility decrease is observed at a similar pressure for both melts, although they are chemically and thermodynamically different. Comparison of the silica and olivine data raises the question of why the absolute Ar solubilities are so different for the two melts at low pressure. The maximum solubility for SiO_2 was 5wt% at 5 GPa, whereas that for molten olivine was 0.2wt% at the same pressure.

Silica is a fully polymerized electrically neutral framework that simply traps the neutral atoms within the melt cages. Olivine forms an ionic liquid, bonded by attractive and repulsive interactions between metal cations (for example Mg^{2+} or Fe^{2+}) and SiO_4^{4-} anions. The average ionic separation should be close to that defined by the minimum-energy configuration. Placing Ar atoms in this liquid causes the ion–ion distance to increase, decreasing the net ionic attraction. Polarization of the rare-gas atoms will cause a further decrease in ion–ion attraction. The result is that the internal energy of the liquid is increased (in other words it becomes less negative). This 'ionic dilution' effect, which destabilizes the liquid thermodynamically, causes less argon to be dissolved in olivine melt than in silica.

This argument predicts that fully polymerized melts should have similar rare-gas solubilities to silica, once account is taken of available site filling by charge-balancing cations. The rare-gas solubility should decrease rapidly as the polymerization decreases. Preliminary data for enstatite and diopside melts support this argument. Ar solubilities in these melts are nearly identical to that in forsterite for pressures below 4 GPa (Fig. 4a). We predict that natural mantle melts have a similar behaviour, with an abrupt decrease in Ar solubility in the 3–5-GPa pressure range. The model can be used to predict the behaviour of other noble gases in mantle melts. It is expected that the solubility decrease would occur below 2 GPa for Xe but not until 8–10 GPa for He, owing to the different sizes of the noble gas atoms (Fig. 3). In our preliminary experiments[9] we obtained one data point for anorthite melt at 10 GPa that did not agree with this model. But those experiments were plagued with problems associated with the incongruent melting of that composition at high pressure, and that solubility determination is unreliable. There are no such problems with silica and forsterite melts because their melting is congruent throughout the pressure range 0–10 GPa.

The sudden decrease in Ar solubility in the melt at 4–5 GPa has important consequences for its geochemical behaviour. It is assumed that noble gases are always strongly incompatible during partial melting, that is, that they are preferentially fractionated into the melt. This assumption is supported by low-pressure (<0.2 GPa) experimental data indicating that the olivine–melt partition coefficient ($K_d = [Ar]_{crystal}/[Ar]_{melt}$) is $\sim 10^{-2}$ (ref. 17). In previous geochemical modelling, it has been implicitly assumed that this value is independent of pressure. However, our data indicate an abrupt decrease in Ar solubility in the melt, by at least one order of magnitude, in the 4–5 GPa range. Unless there is a corresponding change in the crystal solubility at this pressure, which is unlikely, the behaviour of Ar will change from strongly incompatible toward moderately incompatible, or even compatible, if the melt solubility becomes lower than that of the crystal (Fig. 4b) Similar effects are expected at lower pressures for heavy noble gases such as Kr ore Xe, and at higher pressure for He. □

Received 27 June 1997; accepted 9 March 1998.

1. Jambon, A. in *Volatiles in Magmas* (eds Carroll, M. R. and Holloway, J. R.) 479–517 (Mineralogical Soc. Am., Washington DC, 1994).

2. Zhang, Y. & Zindler, A. Noble gas constraints on the evolution of the Earth's atmosphere. *J. Geophys. Res.* **94,** 13719–13737 (1989).
3. Azbel, I. & Tolstikhin, I. N. Geodynamics, magmatism, and degassing of the Earth. *Geochim. Cosmochim. Acta* **54,** 139–154 (1990).
4. Allègre, C., Hofmann, A. & O'Nions, K. The argon constraints on mantle structure. *Geophys. Res. Lett.* **23,** 3555–3557 (1996).
5. Albarède, F. Time-dependent models of U–Th–He and K–Ar evolution and the layering of mantle convection. *Chem. Geol.* (in the press).
6. White, B. S., Brearley, M. & Montana, A. Solubility of argon in silicate liquids at high pressures. *Am. Mineral.* **74,** 513–5229 (1989).
7. Montana, A., Guo, Q., Boettcher, S., White, B. S. & Brearley, M. Xe and Ar in high pressure silicate liquids. *Am. Mineral.* **78,** 1135–1142 (1993).
8. Carroll, M. L. & Stolper, E. M. Noble gas solubilities in silicate melts and glasses: new experimental results for argon and the relationships between solubility and ionic porosity. *Geochim. Cosmochim. Acta* **75,** 5039–5051 (1993).
9. Chamorro-Perez, E., Gillet, P. & Jambon, A. Argon solubility in silicate melts at very high pressures. Experimental set-up and preliminary results for anorthite and silica melts. *Earth Planet. Sci. Lett.* **145,** 97–107 (1996).
10. Wang, S. Y., Sharma, S. K. & Cooney, T. F. Micro-Raman and infrared spectral study of forsterite under high pressure. *Am. Mineral.* **78,** 469–476 (1993).
11. Gillet, P., Fiquet, G., Daniel, I. & Reynard, B. Raman spectroscopy at mantle pressure and temperature conditions. Experimental set-up and the example of $CaTiO_3$ perovskite. *Geophys. Res. Lett.* **20,** 1931–1934 (1993).
12. Ohtani, E. & Kuazawa, M. Melting of forsterite Mg_2SiO_4 up to 15 GPa. *Phys. Earth Planet. Inter.* **27,** 32–38 (1981).
13. Shackelford, J. & Masaryk, J. The interstitial structure of vitreous silica. *J. Non-Cryst. Solids* **30,** 127–139 (1978).
14. Shibata, T., Takahashi, E. & Matsuda, J. Noble gas solubility in binary CaO–SiO_2 system. *Geophys. Res. Lett.* **23,** 3139–3142 (1996).
15. Agee, C. & Walker, D. Static compression and olivine flotation in ultrabasic silicate liquid. *J. Geophys. Res.* **93,** 3437–3449 (1988).
16. Poole, P. H., McMillan, P. F. & Wolf, G. H. in *Structure, Dynamics and Properties of Silicate Melts* (eds Stebbins, J. F., McMillan, P. F. and Dingwell, D. B.) 563–616 (Mineralogical Soc. Am., Washington DC, 1995).
17. Brooker, A., Wartho, J.-A., Carroll, M. & Kelley, P. Preliminary UVLAMP determinations of argon partition coefficients for olivine and clinopyroxene grown from silicate melts. *Chem. Geol.* (submitted).

Acknowledgements. We thank P. Blanc for his assistance with the SEM, D. Badia for help with microprobe analysis and K. Roselieb for giving the Ar–SiO_2 standard. We are grateful to R. A. Brooker for making his manuscript available before publication. This work was financially supported by the INSU program 'DBT: Terre Profonde'.

Correspondence and requests for materials should be addressed to P.G. (e-mail: pgillet@geologie.ens-lyon.fr).

Rare-gas solids in the Earth's deep interior

Andrew P. Jephcoat

Department of Earth Sciences, University of Oxford, Parks Road, Oxford OX1 3PR, UK

Chemical inertness and surface volatility, combined with low abundance, have made the rare (noble) gases a unique trace-elemental and isotopic system for constraining the formation and evolution of the solid Earth and its atmosphere[1–3]. Here I examine the implications of recent high-pressure measurements of the melting temperatures of heavy rare-gas solids—argon, krypton and xenon—with new diamond-anvil cell methods, together with their pressure–volume relationship, for the total rare-gas inventory of the Earth since its formation. The solid–liquid (melting) transition in these rare-gas solids rises significantly with pressure in the 50 GPa range[4,5], such that melting temperatures will exceed the geotherm at pressures of the Earth's transition zone and lower mantle (depths greater than 410–670 km). The densities of condensed rare-gas solids obtained from recent pressure–volume measurements at high compressions also exceed Earth's mantle and core densities. These pressure-induced changes in the physical properties of rare-gas solids, combined with their expected low solubilities and diffusional growth mechanisms, suggest that dense solid or fluid inclusions of rare gases—initially at nanometre scales—would have formed in the Earth's interior and may have resulted in incomplete planetary degassing. Separation of dense solid inclusions into deeper regions during early planet formation could provide a straightforward explanation for the unexpectedly low absolute abundance of xenon observed in the atmospheres of both Earth and Mars.

All the rare gases crystallize under sufficient pressure to form close-packed solids that have been extensively studied with the diamond-anvil cell (DAC). Measured physical properties include the (300 K) equation of state (EOS; pressure–volume relationship), structural phase transitions, insulator–metal transitions and melting. Pressure–volume data to near 130 GPa at 300 K for solid Kr, reported here, complete the measurement of the EOS of the heavy rare gases (Ar, Kr, Xe) in this pressure range (Fig. 1). In addition, the solid–liquid phase transition boundary has been determined to pressures in the range 20–50 GPa (refs 4, 5) with the laser-heated DAC. Ar melting temperatures (T_m) coincide closely[5] with several first-principles calculations to 50 GPa. If these melting temperatures are compared with a recent mantle geotherm based on experimental melting and phase relations in transition zone minerals[6] (Fig. 2), they rise steeply above the geotherm at pressures (depths) around 8 GPa (270 km), 14 GPa (420 km) and 25 GPa (720 km) for Xe, Kr and Ar, respectively. Above these pressures, clusters of rare gas atoms not bound structurally within a host phase in the Earth would be thermodynamically stable in the solid phase. Confidence in the crossing of these melting curves with the geotherm is provided by the experimental observation of the coincidence of the melting curves of solid Ar and Kr with the melting curve of pure iron (Fig. 2) and solid Xe with platinum[5]. The melting curves to core pressures (130 GPa) are less well constrained, but the data indicate that all the rare-gas solids (RGS) should melt at higher temperatures than iron, the dominant core component. A softening of RGS melting curves (a less rapid increase with pressure) may mean that dense rare-gas fluids would be stable near the base of the lower mantle and in the core, depending on

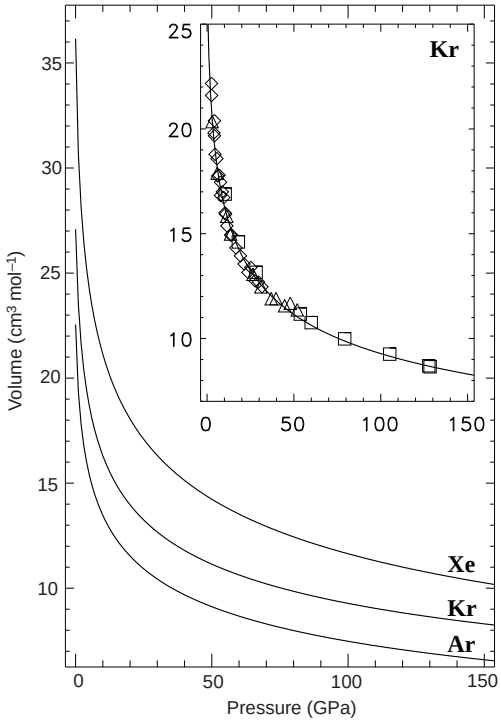

Figure 1 Molar volumes of solid Ar, Kr and Xe as a function of pressure at 300 K from DAC measurements. The solid lines are fits of an EOS using the condensed phase zero-pressure volume at low temperature (Table 1). The inset shows recent *P–V* data for solid krypton collected up to 128 GPa (squares) at Beamline X7A of the National Synchrotron Light Source, with angle-dispersive X-ray diffraction techniques plotted with earlier, independent measurements (triangles and diamonds).